Pharmaceutica Analytica Acta
ISSN: 2153-2435

Srinivasaraghavan et al., Pharmaceut Anal Acta 2017, S8
DOI: 10.4172/2153-2435.S8-002

Research Article Open Access

Experimental and Theoretical Spectroscopic Analysis on N-((1-(phenyl-sulfonyl)-1H-indol-3-Yl)methyl)acetamide

Srinivasaraghavan R[1], Seshadri S[2]*, Gnanasambandan T[3] and Srinivasan G[4]

[1]Department of Physics, SCSVMV University, Kanchipuram-631561, Tamil Nadu, India
[2]Department of Physics, Dr. Ambedkar Govt. Arts College, Chennai-39, Tamil Nadu, India
[3]Department of Physics, Pallavan College of Engineering, Kanchipuram-631502, Tamil Nadu, India
[4]Department of Physics, Government Arts College, Chennai-35, Tamil Nadu, India

Abstract

In this work, The structural characteristics and vibrational spectroscopic analysis were carried out by quantum chemical methods with the hybrid exchange-correlation functional B3LYP using 6-31G (d, p) and 6-311++G (d, p) basis sets in order to investigate the fundamental modes of vibrational analysis and electronic properties of phenyl substituted compound N-((1-(phenylsulfonyl)-1H-indol-3-yl)methyl)acetamide. Density Functional Theory (DFT) method, using B3LYP functional, with 6-31G (d, p) and 6-311++G (d, p) basis sets, which in turn creates a platform to study the structure of the chosen compound. The experimentally obtained FTIR and FT Raman spectrum supports the results of theoretically observed ones. Detailed interpretations of the experimental spectra of the molecule along with the theoretical ones are reported based on Potential Energy Distribution (PED).

The total dipole moment, static total and anisotropy of polarisability and static first hyperpolarisability values were calculated. The FMOs, molecular electrostatic potential, global reactivity descriptors were also calculated and discussed. Molecular electrostatic potential and frontier molecular orbitals were constructed to understand the electronic properties. The intramolecular contacts are interpreted using Natural Bond Orbital (NBO) analysis to ascertain the charge distribution. The thermodynamic properties at different temperatures were calculated revealing the correlations between standard heat capacities, entropy and enthalpy changes with temperatures.

Keywords: N1PS3MA; NBO/NLMO; MEP; PED

Introduction

N-((1-(phenylsulfonyl)-1H-indol-3-yl)methyl)acetamide is basically an indole derivative, otherwise called [N1PS3MA] having molecular formula $C_{16}H_{16}N_2O_3S$. The phenyl sulfonyl ring makes 66.5(7) dihedral angle with the indole unit. Some of the indole alkaloids extracted from plants possess interesting cytotoxic, antitumour or antiparasitic properties [1,2]. Pyrido[1,2-a] indole derivatives have been identified as potent inhibitors of human immunodeficiency virus type-1 [3], and 5-chloro-3-(phenylsulfonyl) indole-2-carboxamide is reported to be a highly potent non-nucleoside inhibitor of HIV-1 reverse transcriptase [4]. The interaction of phenylsulfonylindole with calf thymus DNA has also been studied by spectroscopic methods [5]. The Compound was synthesized one and the molecular parametric details are obtained from the similar compound synthesized by A. Thenmozhi et al. [6] and no further studies have been carried out for the title compound yet. Literature survey reveals that so far no spectroscopic and computational work was carried out on the title compound. Therefore in our present investigation, the spectroscopic properties of N-((1-(phenylsulfonyl)-1H-indol-3-yl)methyl)acetamide were studied by vibrational spectroscopy (FT-IR, FT-Raman) and additionally the structure, vibrational frequencies and other thermodynamical parameters of the title molecule were calculated by the DFT method. The redistribution of electron density (ED) in various bonding and antibonding orbitals and E(2) energies have been calculated by Natural Bond Orbital (NBO/NLMO) analysis using DFT method to give clear evidence of stabilization originating from the hyperconjugation of various intramolecular interactions. The HOMO and LUMO analysis have been used to elucidate the information regarding charge transfer occurs within the molecule. Moreover, the Mulliken population analyses of the title compound have been calculated and the calculated results have been reported.

Experimental

The compound N-((1-(phenylsulfonyl)-1H-indol-3-yl)methyl) acetamide [N1PS3MA] was a synthesized one and reported in Literature [6] and used as such without further purification to record FTIR and FT Raman spectra. The FTIR spectrum of the compounds is recorded in the region 4000- 400 cm^{-1} in evacuation mode on Bruker IFS 66V spectrophotometer using KBr pellet technique (solid phase) with 4.0 cm^{-1} resolutions. The FT-Raman spectra of these compounds are also recorded in the same instrument with FRA 106 Raman module equipped with Nd: YAG laser source operating at 1.064 μm line widths with 200 mW powers. The spectra are recorded in the range of 3500–100 cm^{-1} with scanning speed of 30 cm^{-1} min^{-1} of spectral width 2 cm^{-1}. The frequencies of all sharp bands are accurate to ± 1 cm^{-1}. The spectral measurements were carried out at Sophisticated Analytical Instrumentation Facility, IIT, Chennai, Tamil Nadu, India.

Methods of Analysis

The optimized molecular geometrical orientation and the vibrational frequency calculations are carried out for N1PS3MA, with the Gaussian 03W software package [7]. Becke's three parameter

***Corresponding author:** Seshadri S, Department of Physics, Dr. Ambedkar Govt. Arts College, Vyasarpadi, Chennai-39, Tamil Nadu, India, Tel: 0866-2497299, E-mail: sri_sesha@yahoo.com

Received June 15, 2017; **Accepted** August 02, 2017; **Published** August 07, 2017

Citation: Srinivasaraghavan R, Seshadri S, Gnanasambandan T, Srinivasan G (2017) Experimental and Theoretical Spectroscopic Analysis on N-((1-(phenyl-sulfonyl)-1H-indol-3-Yl)methyl)acetamide. Pharmaceut Anal Acta S8. doi:10.4172/2153-2435.S8-002

exchange functional (B3) [8] and combination with the correlation functional of Lee, Yang and Parr (LYP) [9] were adopted with standard 6-31G(d,p) and 6-311++G (d,p) basis sets. The optimized geometrical parameters namely, bond length and bond angles calculated by two basis sets are listed in Table 1 along with the experimental data on the geometric structure of the selected molecule. This molecule has fifteen

Molecular parameters/ Bond lengths	Experimental	B3LYP/6-31G(d,p)	B3LYP/6-311++G(d,p)
H(39)-C(23)	1.100	1.101	1.101
H(38)-C(22)	1.100	1.101	1.092
H(37)-C(21)	1.100	1.101	1.096
H(36)-C(20)	1.100	1.101	1.096
H(35)-C(19)	1.100	1.104	1.092
H(34)-C(13)	1.100	1.099	1.101
H(33)-C(12)	1.100	1.099	1.091
H(32)-C(11)	1.100	1.099	1.102
H(31)-C(10)	1.100	1.112	1.097
H(30)-C(7)	1.100	1.089	1.092
H(29)-C(5)	1.113	1.131	1.113
H(28)-C(5)	1.113	1.131	1.094
H(27)-N(4)	1.012	1.081	1.039
H(26)-C(2)	1.113	1.118	1.116
H(25)-C(2)	1.113	1.116	1.117
H(24)-C(2)	1.113	1.116	1.117
C(23)-C(18)	1.337	1.403	1.402
C(23)-C(22)	1.337	1.396	1.331
C(22)-C(21)	1.337	1.398	1.331
C(21)-C(20)	1.337	1.397	1.335
C(20)-C(19)	1.337	1.398	1.382
C(19)-C(18)	1.337	1.404	1.376
C(18)-S(15)	1.790	1.731	1.746
O(17)-S(15)	1.450	1.422	1.45
O(16)-S(15)	1.450	1.425	1.451
S(15)-N(6)	1.696	1.654	1.701
C(14)-N(6)	1.396	1.406	1.401
C(14)-C(13)	1.337	1.416	1.381
C(14)-C(9)	1.337	1.439	1.381
C(13)-C(12)	1.337	1.39	1.381
C(12)-C(11)	1.337	1.409	1.389
C(11)-C(10)	1.337	1.386	1.372
C(10)-C(9)	1.337	1.395	1.356
C(9)-C(8)	1.337	1.456	1.396
C(8)-C(7)	1.337	1.386	1.362
N(6)-C(7)	1.401	1.388	1.401
C(8)-C(5)	1.497	1.506	1.494
C(5)-N(4)	1.450	1.444	1.441
N(4)-C(1)	1.369	1.381	1.389
O(3)-C(1)	1.208	1.251	1.247
C(2)-C(1)	1.509	1.516	1.509
Bond angles (°)			
H(39)-C(23)-C(18)	120.0	120.2	120.1
H(39)-C(23)-C(22)	120.0	118.8	119.9
C(18)-C(23)-C(22)	120.0	121.0	119.5
H(38)-C(22)-C(23)	120.0	120.1	120.0
H(38)-C(22)-C(21)	120.0	119.9	120.0
C(23)-C(22)-C(21)	120.0	120.0	120.0
H(37)-C(21)-C(22)	120.0	120.1	120.1
H(37)-C(21)-C(20)	120.0	120.2	120.0
C(22)-C(21)-C(20)	120.0	119.7	119.9
H(36)-C(20)-C(21)	120.0	119.8	119.9
H(36)-C(20)-C(19)	120.0	120.2	119.2
C(21)-C(20)-C(19)	120.0	120.0	120.9
H(35)-C(19)-C(20)	120.0	119.2	119.7
H(35)-C(19)-C(18)	120.0	119.8	120.3
C(20)-C(19)-C(18)	120.0	121.0	120.7
S(15)-C(18)-C(23)	120.0	121.1	119.1
S(15)-C(18)-C(19)	120.0	118.5	119.5
C(23)-C(18)-C(19)	120.0	118.3	119.1
O(16)-S(15)-O(17)	109.5	117.2	117.7
O(16)-S(15)-N(6)	109.4	110.3	108.8
O(16)-S(15)-C(18)	109.5	106.5	110.1
O(17)-S(15)-N(6)	109.4	108.8	109.0
O(17)-S(15)-C(18)	109.5	109.6	110.2
N(6)-S(15)-C(18)	109.5	108.6	110.2
N(6)-C(14)-C(13)	122.0	121.1	120.4
N(6)-C(14)-C(9)	120.0	109.3	119.3
C(13)-C(14)-C(9)	120.0	118.6	119.8
H(34)-C(13)-C(14)	120.0	120.9	119.7
H(34)-C(13)-C(12)	120.0	120.2	119.8
C(14)-C(13)-C(12)	120.0	119.0	121.7
H(33)-C(12)-C(13)	120.0	119.0	119.2
H(33)-C(12)-C(11)	120.0	118.9	119.6
C(13)-C(12)-C(11)	120.0	122.1	121.1
H(32)-C(11)-C(12)	120.0	121.2	120.9
H(32)-C(11)-C(10)	120.0	119.4	120.4
C(12)-C(11)-C(10)	120.0	119.4	120.3
H(31)-C(10)-C(11)	120.0	122.7	118.8
H(31)-C(10)-C(9)	120.0	115.1	118.3
C(11)-C(10)-C(9)	120.0	120.3	120.9
C(8)-C(9)-C(14)	111.0	106.0	109.3
C(8)-C(9)-C(10)	120.0	121.4	120.5
C(14)-C(9)-C(10)	120.0	120.6	120.1
C(5)-C(8)-C(7)	120.9	121.2	120.3
C(5)-C(8)-C(9)	124.5	124.8	124.5
C(7)-C(8)-C(9)	111.0	106.0	108.1
C(8)-C(7)-H(30)	129.5	129.5	129.4
C(14)-N(6)-S(15)	127.0	125.4	124.9
C(7)-N(6)-C(14)	121.9	121.3	121.6
C(7)-N(6)-S(15)	127.1	128.1	126.2
N(4)-C(5)-C(8)	109.5	113.9	109.0
N(4)-C(5)-H(28)	109.4	108.1	108.9
N(4)-C(5)-H(29)	109.5	108.2	110.8
C(8)-C(5)-H(28)	109.4	109.2	110.7
C(8)-C(5)-H(29)	109.5	109.4	109.6
H(28)-C(5)-H(29)	109.5	107.9	109.3
C(1)-N(4)-C(5)	120.0	126.0	121.4
C(1)-N(4)-H(27)	120.0	120.8	120.3
C(5)-N(4)-H(27)	120.0	121.2	120.6
C(1)-C(2)-H(24)	109.5	113.8	111.1
C(1)-C(2)-H(25)	109.4	108.5	110.5
C(1)-C(2)-H(26)	109.5	108.4	110.5
H(24)-C(2)-H(25)	109.4	108.5	110.6
H(24)-C(2)-H(26)	109.5	108.4	110.3
H(25)-C(2)-H(26)	109.5	109.1	109.1
C(2)-C(1)-O(3)	120.0	122.1	121.1
C(2)-C(1)-N(4)	120.0	115.6	121.4
O(3)-C(1)-N(4)	120.0	122.3	120.8
N(6)-C(7)-C(8)	123.1	121.4	121.3
N(6)-C(7)-H(30)	121.9	118.1	119.3

Table 1: Molecular geometrical parameters of N-((1-(phenylsulfonyl)-1H-indol-3-yl)methyl)acetamide N1PS3MA.

C-H bond lengths, seventeen C-C bond lengths, four C-N bond lengths, two S-O bond lengths, one C-S and N-S bond length, and a C-O bond length. The C-C bond length value of the ring is found to be 1.337 Å at B3LYP/6-311++G (d,p) level. The C-O bond length value is found to be 1.208 Å. The C-H bond length value calculated at B3LYP/6-311++G (d,p) level vary from 1.096 to 1.101 Å and the N-H bond length value is 1.411 Å. Here the value of S-C bond length is found to be high compared to other bond length values. The calculated bond angles of C-C-H, C-C-C, O-C-H and H-C-H are found to be slightly on the higher side compared to experimental values of bond angle. The Cartesian representation of the theoretical force constants have been computed at the optimized geometry by assuming C_1 point group symmetry. The vibrational wavenumbers are calculated with PED calculations at the optimized geometrical orientation. The atomic charges, electric dipole moment, polarizability, first hyperpolarizability, HOMO, LUMO and thermodynamic parameters are also calculated theoretically. The Natural Bonding Orbital (NBO) calculations are performed using NBO 3.1 program as implemented in the Gaussian 03W [7] package at DFT level in order to understand various second-order interactions between the filled orbital of subsystem and vacant of another subsystem, which is a measure of the intermolecular delocalization or hyperconjugation. Finally, the calculated normal mode of vibrational frequencies will provide the thermodynamic properties using the principle of statistical mechanics. The optimized structure of N1PS3MA is shown in Figure 1.

Vibrational assignments

The title molecule consists of 39 atoms, hence (3N-6) gives 111 normal modes of vibrations, and all are active in infrared and Raman spectra. The detailed vibrational assignments of fundamental modes along with the calculated IR, Raman intensities and normal mode description (characterized by PED) are reported in Table 2. For comparison, the observed and simulated Raman and IR spectra are presented in Figures 2 and 3.

CH_2 and CH_3 vibrations: There is one CH_3 and a CH_2 group in this compound. Earlier researchers [10,11] have reported infrared bands occurring in the range 3100-2900 cm^{-1} as due to C-H stretching in their study. The assignments of CH_2 group frequency involve six fundamentals namely, CH_2 symmetric stretch; CH_2 asymmetric stretch; CH_2 scissoring and CH_2 rocking which belongs to in-plane vibration and out of plane vibration namely CH_2 wagging and CH_2 twisting modes. The fundamental CH_2 vibrations due to scissoring, wagging, twisting and rocking appear in the region 1500–800 cm^{-1}. The asymmetric CH_2 stretching vibrations are generally observed in the region 3200 - 3050 cm^{-1}, while the symmetric stretching will appear between 3050 and 2900 cm^{-1} [12-14]. In this compound the asymmetric stretching of CH_2 vibration occurs at 3177 cm^{-1} in FTIR and 3175 cm^{-1} in FT Raman spectra. The symmetric stretching vibrations occur at 3059 cm^{-1} in FTIR and in FT Raman spectra. The results of symmetric and asymmetric CH_2 vibrations agree well with the DFT method.

CH_2 scissoring is assigned to 1492, 1410 cm^{-1} in experimental observation agrees the values at 1492, 1410 cm^{-1} in B3LYP method. CH_2 wagging is attributed to 1392 cm^{-1}, 1381 cm^{-1} in FTIR, and the corresponding values in FT-Raman are in good agreement B3LYP values. Emilio et al. have observed CH_3 scissoring at 1513 cm^{-1} and based on this reference, in our compound the band at 1501 cm^{-1} is assigned to CH_3 scissoring and CH_2 wagging is assigned to the band at 1365 cm^{-1} in both FTIR and FT-Raman spectra [15].

The title compound has one CH_3 group. The asymmetric CH_3 is expected around 3187 cm^{-1} and CH_3 symmetric stretching is expected at 3073 cm^{-1} [16,17]. In this study apart from CH_2 and CH_3 the other CH asymmetric and symmetric stretching vibrations are identified in their respective ranges and these results agree well with the values of DFT method.

N-H vibrations: Normally the vibrational bands due to the N-H stretching are sharp by virtue of which they can be easily identified. Tsuboi [18] reported the N-H stretching frequency at 3481 cm^{-1} in aniline. In our study the band appear at 3460 and 3461 cm^{-1} in the FTIR and FT Raman spectrum is assigned to N-H stretching vibrations. The theoretically calculated value by DFT method at 3459 cm^{-1} shows agreement with experimentally observed value. Though the identification of bands is difficult, with the help of the animation

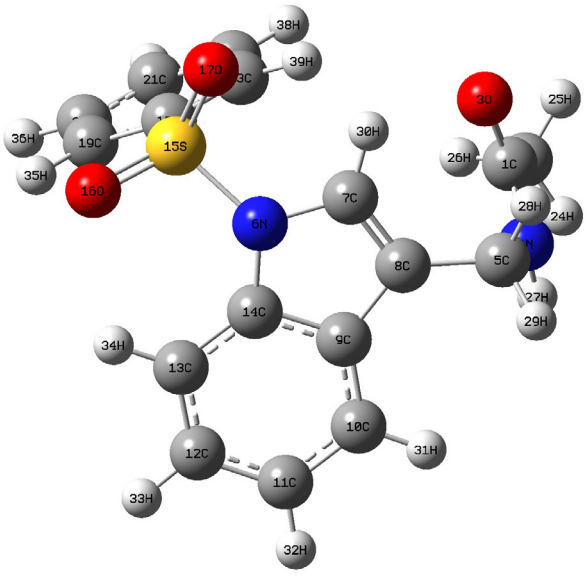

Figure 1: Optimised structure of N-((1-(phenylsulfonyl)-1H-indol-3-yl)methyl)acetamide.

FTIR v_{IR} cm^{-1}	FT Raman v_R cm^{-1}	B3LYP/6-31G(d,p)			B3LYP/6-311++G(d,p)			Assignments with PED % calculation
		v_{cal} cm^{-1}	IR intensity	Raman activity	v_{cal} cm^{-1}	IR intensity	Raman activity	
		20	0.323	2.789	19	1.221	1.404	α ring scissoring (15)
		25	2.441	1.833	24	1.008	9.701	τ ring (12)
		32	0.707	10.770	32	0.586	5.473	β ring (16)+γSO_2(wag) (28)
		48	0.240	6.500	47	1.763	5.022	α ring (10)
		56	5.021	6.753	56	1.432	1.70	γCH_3(wag) (16)
		74	16.795	0.571	75	6.403	3.70	τCH_3(10)+γSO_2(wag) (19)
		85	0.089	0.293	83	1.38	8.479	γCH_3(wag) (25)
	113	115	1.270	0.477	113	0.45	6.769	γCO(12)+γNH(16)
	141	138	1.836	2.153	139	1.582	4.843	τCH(10)+τSO_2 (23)
	147	145	4.598	1.900	144	2.960	0.754	α C N (27)+γCH (16)
		164	1.945	1.407	164	1.807	2.190	τCH(12)+βCH_3(34)
	179	178	0.576	2.023	178	0.948	0.56	τCH_3 (24)
	226	222	2.027	3.754	221	1.600	0.857	β CN (27)+γCH (11)
		248	1.811	1.348	249	2.244	0.816	α CH(16)+α CH_3(14)
	280	279	4.354	3.16	279	3.541	2.806	βNCC(13)
		285	0.132	6.045	286	3.89	0.685	α CH(14)+α CH_2(25)+ α CH_3(13)
	297	296	0.338	1.471	298	3.009	4.830	τCH_2 (15)
	310	307	1.387	4.166	308	9.148	3.536	βCCC(37)+α NH(18)+α CH_3(34)
		316	3.901	5.285	317	4.043	6.435	νCC(14)+βring(26)
	365	363	3.240	0.589	363	0.054	0.487	γ ring 1 (12)
	401	403	9.417	2.96	404	8.240	1.504	τCH_3 (41)+α NH(10)
412		412	19.862	1.263	412	0.486	2.664	τring (19)+βCCC (24)
421	421	421	0.171	0.264	422	9.892	4.194	α SO_2(20)+α CH_3(32)
435		436	3.468	0.413	439	66.473	2.867	α CH(24)+α NH(14)+α CH_2(36)
466	465	467	15.884	1.034	467	23.901	2.162	γCN (21)+βring (19)
489	487	485	4.964	5.145	486	83.144	13.301	γring 4 (53)+γCS (26)
537		536	1.237	3.037	536	89.263	1.692	τ ring (25)+γCH(19)
	543	545	49.015	1.275	544	68.808	3.132	δNS (37) δring 4 (26)
565	565	564	83.825	2.191	565	18.708	0.329	τNC(22)+βCCO(20)
577		576	81.884	2.600	574	61.412	87.798	α CH(12)+α SO_2(36)+α CH_3(18)
594	593	594	16.396	0.647	597	12.41	39.439	νCS (58)
	607	607	17.129	4.404	607	38.552	1.29	γCO(27)+τNC(14)
615	616	616	80.291	11.37	618	65.291	1.815	γNH (52)
627	628	626	3.573	4.454	627	0.266	1.146	α CH(27)+α CH_3(43)
655		657	7.028	2.179	658	1.45	1.244	γCC(23)+α NH(15)
688	687	685	2.507	6.313	683	89.358	5.227	α CH(27)+γCN(31)
700	701	699	38.888	1.520	700	89.053	1.994	βCCN(33)
721	723	723	42.540	4.078	722	118.28	4.008	α CH(10)+δCH(19)
738	739	740	36.885	3.722	741	9.108	12.968	βNCH(18)
764	762	763	50.370	2.216	763	96.184	11.369	νCS (68)+δCH(12)
767		766	10.311	5.73	767	3.718	5.694	γCC(17)
778	779	780	11.655	11.90	779	78.261	2.105	γCH(26)+νCS (52)
793	791	791	34.742	0.755	792	79.704	29.146	γCH(86)+δCH(12)
840	841	843	9.146	11.338	843	62.076	32.832	γCN(8)+α CH_2(18)
860	859	859	1.339	3.920	859	0.344	3.122	βring(27)
866		865	1.460	3.625	866	90.347	4.019	α CH(26)+γCH (39)
877	876	875	1.483	3.326	875	8.131	1.873	γCN(10)
939	939	942	1.322	0.304	945	7.926	3.195	γCH(29)+νCC(75)
951	952	952	1.368	0.779	952	4.830	1.704	γCC(36)+τring(13)
960		961	54.017	5.533	962	8.460	2.998	γCH (46)
982	982	983	0.662	0.124	981	0.136	0.975	γSO(35)+α CH_3(32)
987		986	2.980	2.592	985	0.496	1.778	νCN(27)+νCC(51)
	988	987	0.223	0.781	989	11.544	7.389	γCN(25)
998	998	997	0.156	0.171	998	39.504	1.876	α CH_3(48)+α CH_2(15)
1010	1011	1010	4.304	20.167	1011	19.105	0.880	γCH(31)+γCC(17)

1014		1013	5.019	1.482	1015	33.371	0.14	α CH(82)
1030	1030	1029	3.264	9.970	1031	27.248	0.308	γCH(27)+βNCH(15)
1045	1045	1047	9.149	30.487	1046	9.167	3.667	α CH_3(48)
1053		1051	10.234	0.628	1051	5.30	16.682	vCC(58)+βCCH(11)
1059	1059	1058	14.259	4.277	1060	6.5058	3.047	γCO(16)+vCN(63)
1082	1082	1083	52.544	6.016	1084	41.659	7.828	CH_3(48)+α NH(12)
1090	1090	1089	14.801	6.129	1090	0.877	36.190	βNCH(21)+βring(18)
1109	1110	1107	6.206	0.464	1107	47.77	27.369	δSO (42)
1114		1113	83.117	4.395	1112	1.974	20.088	α CH(65)
1139	1139	1138	76.828	38.985	1138	3.191	6.124	βCCH(16)
1154	1153	1153	41.620	7.384	1155	9.916	2.805	α CH(83)
1159	1159	1158	0.263	5.652	1160	19.235	2.443	βNCH(21)
	1190	1190	14.053	1.708	1189	0.814	5.201	v CC(72)
1192		1191	0.237	5.448	1192	12.360	7.885	v CN (79)
1211	1211	1210	29.888	8.555	1214	0.859	1.774	α CH_2(27)+vCN (58)
1243	1243	1242	11.162	7.103	1245	35.552	8.144	v CN (64)+δCH (53)$_+v_s$SO (67)
1260		1260	17.425	5.235	1261	6.130	12.543	α CH_2(19)+α NH(38)+vSO_2 (61)
1293	1294	1293	27.507	19.927	1293	0.838	52.282	vCN(70)+vSO_2 (59)+τCH_3(44)
1310		1307	7.081	20.766	1305	15.639	10.117	τCC (33)+vSO_2 (58)
1319	1319	1319	1.161	0.433	1320	4.864	62.133	vCC (92)+v_aSO(78)
1342	1342	1341	18.645	3.235	1342	9.981	55.413	vCC (88)+βCCO(11)
1351	1351	1351	15.587	1.280	1354	24.991	36.373	βCCH(28)+vCC(84)
1366	1365	1366	2.151	28.067	1368	15.263	10.439	vCC(76)+α CH_3(42)
1381	1381	1381	22.095	17.860	1383	40.296	54.424	vCC(69)+σCH_2(13)
1392		1392	3.276	25.830	1392	8.968	21.589	vCC(59)+βCCH(33)+σCH_2(17)
1408	1408	1407	19.935	9.575	1405	29.521	28.042	vCN(61)+βCCH(33)
1410		1410	42.073	8.629	1409	31.733	5.515	vCC(62)+α CH_3(18)+α CH_2(52)
1446	1446	1445	12.640	12.889	1447	55.399	28.687	vCC(75)+βHCH(13)
1477	1479	1480	19.743	11.107	1480	11.536	8.412	vCN(57)+βCCC(34)
1485		1483	19.696	5.38	1484	78.601	0.981	vCC(54)+βCCH(33)
	1487	1486	12.449	13.759	1487	49.737	3.491	vCC(67)+α CH_3(28)
1492	1492	1492	4.139	6.625	1489	7.808	2.323	α CH_2(34)+βHCH(13)
1501	1502	1500	3.612	1.36	1501	97.904	3.351	α CH_3(47)+vCC(86)
1518		1518	74.569	2.762	1517	15.040	13.780	γCH(31)
1522	1521	1521	5.562	56.675	1521	39.928	6.329	γCH(29)
1542		1542	5.502	25.20	1541	18.558	11.265	γNH(23)+HCH(52)
1557	1557	1556	0.669	32.009	1559	96.708	3.386	δCH(42)+βCCH(23)
	1572	1573	0.141	13.810	1577	12.07	15.154	δCH(17)
1587		1587	6.954	22.434	1587	14.92	2.408	δCH(27)
1610	1610	1613	99.064	1.307	1612	99.446	10.575	vCO(85)
3059	3059	3057	6.659	109.15	3060	8.4751	18.816	$v_s$$CH_2$(90)
3073	3073	3074	35.228	116.72	3072	8.1967	2.557	$v_s$$CH_3$(85)
3097	3101	3098	14.246	38.912	3098	12.005	71.489	$v_s$$CH_3$ (90)
3142	3141	3140	4.773	54.682	3142	9.0904	55.287	$v_{as}$$CH_3$ (83)
3154	3152	3154	7.492	79.984	3154	50.940	0.863	$v_{as}$$CH_3$ (89)
3177	3175	3176	7.008	59.638	3175	35.050	4.392	$v_{as}$$CH_2$(90)
3187		3189	1.026	55.803	3187	9.3773	26.404	$v_{as}$$CH_3$(99)
3192	3193	3190	16.385	93.665	3193	39.086	24.708	vCH(94)
3200	3199	3202	13.180	100.49	3200	14.099	65.217	vCH(96)
3205		3205	25.436	231.40	3205	26.684	80.673	vCH(99)
3211	3210	3210	12.756	159.73	3211	63.223	29.248	vCH(92)
3222		3225	2.541	72.83	3225	76.555	28.021	vCH(95)
3229	3231	3231	3.190	75.885	3230	76.029	26.494	vCH(98)
3240		3239	1.540	77.343	3239	33.335	98.316	vCH(93)
3299	3300	3301	12.302	37.116	3300	37.822	66.944	vCH(99)
3461	3460	3457	17.427	48.729	3459	61.024	13.574	vNH(98)

v: Stretching; δ: Bending vibrations; γ: In-plane bending; α: Out-of-plane bending; τ: Torsion

Table 2: Vibrational assignments of N1PS3MA using B3LYP/6-31 G(d,p) and B3LYP/6-311++G(d,p).

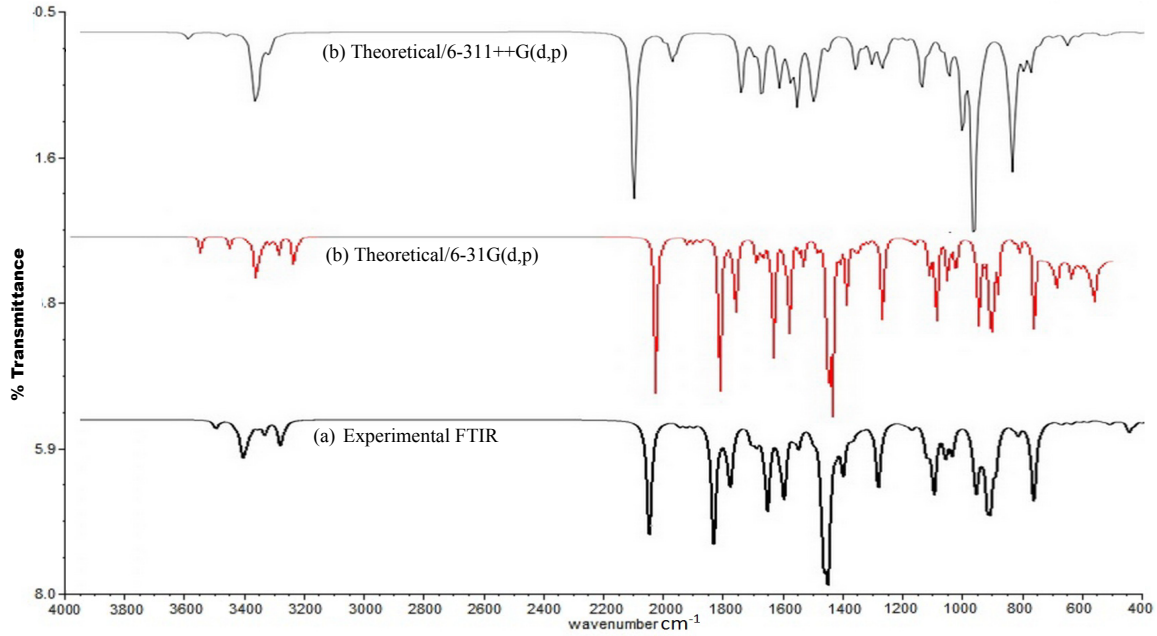

Figure 2: (a) Experimental, and (b) Theoretically simulated IR spectra of N-((1-(phenylsulfonyl)-1H-indol-3-yl)methyl)acetamide.

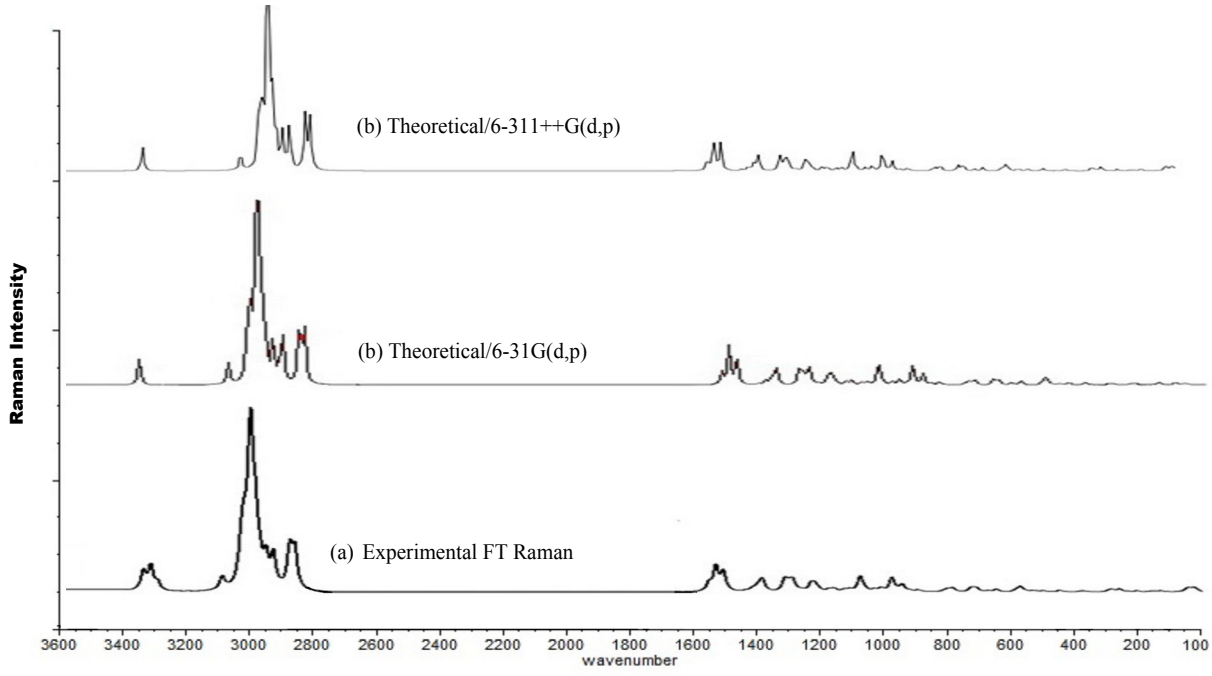

Figure 3: (a) Experimental, and (b) Theoretically simulated Raman spectra of N-((1-(phenylsulfonyl)-1H-indol-3-yl)methyl)acetamide.

option of chemcraft graphical interface for Gaussian programs, the N-H vibration is identified.

C-N vibrations: The identification of C-N vibrations is a very difficult task, since mixing of several bands are possible in this region. The conjugated C-N linkage in amine group gives rise to medium to weak bands near 1350-1150 cm^{-1} because of C-N stretching vibration. Silverstein have assigned C-N stretching absorption in the region 1300-800 cm^{-1}. Gnanasambandan et al. have identified in m-nitromethyl benzoate 1290, 1400 and 1420 cm^{-1} as C-N stretching vibrations. C–N stretching absorption in the region 1382-1266 cm^{-1} for aromatic amines. In our present work 1408, 1294, 1243, 1211 cm^{-1} in FT-IR and 1408, 1293, 1243 and 1211 cm^{-1} in FT-Raman are assigned to C-N stretching. The B3LYP values 1242, 1210, 1191 cm^{-1} corresponds to C-N stretching vibration. Our assignment is in good agreement with the literature [19-24].

C=O vibrations: The carbonyl group shows a strong absorption band due to C=0 stretching vibrations and is observed in the region 1850-1550 cm^{-1}. Because of its high intensity and relatively interference free region in which it occurs, this band is reasonably easy to recognize [25-29]. In the present work the bands observed at 1610 cm^{-1} in FTIR and FT Raman spectrum is assigned to C=O stretching mode of vibration, and it well agrees with the values of DFT method.

C-S vibrations: In general the assignment of the band due to C-S stretching vibration in a compound is difficult. Since it is of variable intensity and may be found over the wide region 1035–245 cm^{-1} both in aliphatic and aromatic sulfides have a weak to medium band due to C-S stretching vibration in the region 710–570 cm^{-1} [30]. In the present work the band observed at 764cm^{-1} in FTIR and 762 cm^{-1} in FT Raman are assigned to C-S stretching vibration. Theoretically computed values are found to be in good agreement with the experimental results.

SO_2 vibrations: Seshadri et al. [31] have reported SO vibrations in 1338 cm^{-1}, 1226 cm^{-1}, and 1217 cm^{-1} in FTIR spectrum. The wavenumbers at 1310 cm^{-1} and 1293 cm^{-1} in FTIR spectrum is assigned to SO_2 asymmetric stretching vibration. The corresponding B3LYP values are 1307 and 1293 cm^{-1}. B3LYP values are in good agreement with the experimental values. The symmetric and asymmetric SO_2 stretching vibrations occur in the region 1125–1260 cm^{-1} and 1260–1330 cm^{-1} respectively. In the title molecule, SO_2 symmetric stretching is observed at 1260 cm^{-1} in FTIR and in FT-Raman. The calculated B3LYP values are 1260 cm^{-1}. The values are in good agreement with the literature.

NBO/NLMO analysis

NBO (natural bond orbital) analysis provides an efficient method for studying intra- and intermolecular bonding and interaction among bonds. It also provides a convenient basis for the investigation of charge transfer or conjugative interactions in molecular system [32]. Another useful aspect of NBO method is that it gives information about interactions in both filled and virtual orbital spaces that could enhance the analysis of intra and intermolecular interactions. The second order Fock matrix was carried out to evaluate the donor–acceptor interactions in the NBO analysis. For each donor NBO (i) and acceptor NBO (j), the stabilization energy associated with ij delocalization can be estimated as:

$$E^{(2)} = \Delta E_{ij} = q_i \frac{F(i,j)^2}{\varepsilon_j - \varepsilon_i}$$

Where q_i is the donor orbital occupancy, are ε_i and ε_j diagonal elements and F (i, j) is the off diagonal NBO Fock matrix element.

In Table 3, the perturbation energies of significant donor–acceptor interactions are presented. The larger the $E^{(2)}$ value, the intensive is the interaction between electron donors and electron acceptors. In N1PS3MA, the interactions between the anti bonding orbitals C18–C23→C21–C22 and C18–C23→C19C20 have the highest $E^{(2)}$ value around 200.25 and 186.87 kcal/mol. The other significant interactions gives stronger stabilization energy values of 171.92 kcal/mol to the structure are the interaction between anti bonding orbital of C7–C8→C9–C14.

The natural localized molecular orbital (NLMO) analysis has been carried out since they show how bonding in a molecule is composed from orbitals localized on different atoms. The derivation of NLMOs from NBOs give direct insight into the nature of the localized molecular orbital's "delocalization tails" [33,34]. Table 3 shows significant NLMO's percentage from parent NBO and atomic hybrid contributions of N1PS3MA calculated at B3LYP level using 6-311++G (d,p) basis set. The NLMO of first lone pair of nitrogen atom N6 is the most delocalized NLMO and has only 82% contribution from the localized LP(1) N6 parent NBO, and the delocalization tail (~16%) consists of the hybrids of C14 and C9.

Electrostatic Potential (ESP)

Molecular Electrostatic Potential (ESP) at a point in the space around a molecule gives an indication of the net electrostatic effect produced at that point by the total charge distribution (electron+nuclei) of the molecule and correlates with dipole moments, electronegativity, partial charges and chemical reactivity of the molecules. It provides a visual method to understand the relative polarity of the molecules. An electron density isosurface mapped with electrostatic potential surface depicts the size, shape, charge density and site of chemical reactivity of the molecules. The different values of the electrostatic potential represented by different colors; red represents the regions of the most negative electrostatic potential, blue represents the regions of the most positive electrostatic potential and green represents the region of zero potential. Potential increases in the order red<orange<yellow<green<blue. Such mapped electrostatic potential surfaces have been plotted for title molecules in 6-311++G(d,p) basis set using the computer software Gauss view. Projections of these surfaces along the molecular plane and a perpendicular plane are given in Figure 4 for N1PS3MA. The Figure 4 provides a visual representation of the chemically active sites and comparative reactivity of atoms.

It may see that, in the molecules, a region of zero potential envelopes the p-system of the aromatic rings, leaving a more electrophilic region in the plane of hydrogen atoms. The shapes of the electrostatic potential at sites close to the polar group in the two molecules. The nitrogen group in the molecules is influenced by the stereo structure and the charge density distribution. These sites show

Donor	Acceptor	$E^{(2)}$ kJ/mol	% from parent NBO	Hybrid atoms
σ(N4−H27)	σ*(C10−H31)	25.97	97.30	H_{31}, H_{32}
π(C9−C14)	π*(C7−C8)	26.81	96.96	H_{31}, H_{34}
σ(C10−H31)	σ*(N4−H27)	94.11	93.31	N_4, C_9
LP(1)N4	π*(C1−O3)	64.08	86.00	C_1, O_3
LP(1)N6	π*(C9−C14)	50.68	81.47	C_7, C_8, C_9, C_{14}, S_{15}
LP(1)O17	σ*(N6−S15)	28.09	89.96	S_{15}, O_{16}, C_{18}
π*(C7−C8)	π*(C9-C14)	171.92	98.62	C_{10}, H_{32}
π*(C18−C23)	π*(C19−C20)	186.87	85.50	C_{12}, H_{33}
π*(C18−C23)	π*(C21−C22)	200.25	93.31	C_{19}, H_{35}

Table 3: Occupancy, percentage of p character of significant natural atomic hybrid of the natural bond orbital, Significant of NLMO's and second Perturbation theory analysis of N1PS3MA calculated at B3LYP/6-311++G(d,p).

regions of most negative electrostatic potential and high activity of the nitrogen groups. In contrast, regions close to the other polar atom-oxygen of the aromatic ring show regions of mildly negative and zero potential, respectively [35].

Mulliken analysis

The atomic charges at all the exocyclic atoms are in accordance with their electro-negativity whereas the charges at all the C atoms of the ring are in accordance with the net flow of p electrons(delocalization of electron density) [36]. The Mulliken atomic charges at each atomic site of N1PS3MA is collected in Table 4 and displayed in Figure 5 along with atom numbering.

According to our calculation the negative charge in an investigated molecule is delocalized between nitrogen and oxygen atoms. The charges calculated for nitrogen atoms are different but the oxygen atoms (O(16) and O(17)) are having same charges (−0.533respectively). The charge on the O16 and O17 atom are found to be equal as they experience the same environment. This depreciation of the negative charges on the oxygen atom may be due to delocalization through the p−electron system of the pyrazole. The positive charges are localized on the hydrogen atoms. The charges on hydrogen's H24, H25and H26 are found to be 0.108, 0.145 and 0.147 respectively and the differences in calculated charges are relatively small. For better visualization, the charge and atom graph is plotted for each charged atom and is displayed in the Figure 6.

Electron density analysis

An analysis of the electron density of highest occupied molecular orbitals (HOMO) and lowest unoccupied molecular orbitals (LUMO) of N1PS3MA can give us some idea about the ground and excited state proton transfer processes. The energies corresponding to HOMO and LUMO levels of N1PS3MA are performed by density functional method. The HOMO–LUMO energy calculation reveals that, there are 86 occupied and 429 unoccupied molecular orbitals associated with N1PS3MA. The energies corresponding to the highest occupied and lowest unoccupied molecular orbitals of N1PS3MA are found to be -5.886 and -1.2547 eV respectively as shown in Table 5. The energy gap between occupied and unoccupied molecular orbitals of N1PS3MA calculated at B3LYP/6-311++G (d,p) level is given in Table 5 reflects the chemical reactivity of the molecule. LUMO as an electron acceptor represents the ability to obtain an electron. HOMO represents the ability to donate an electron.

HOMO orbital on the aromatic ring of N1PS3MA (Figure 7) is primarily of anti-bonding character type over C1, C7, C8 atoms, whereas C2, C5, C10 and N4, N6 show bonding character. Both the hydroxyl and carbonyl oxygen having bonding character type, with a larger electron density over hydroxyl oxygen [37-39]. By using the HOMO and LUMO energy values, the global chemical reactivity descriptors of molecules such as hardness (), chemical potential (μ), softness (S) and electrophilicity index (χ) are calculated using the standard formulas and are defined as follows.

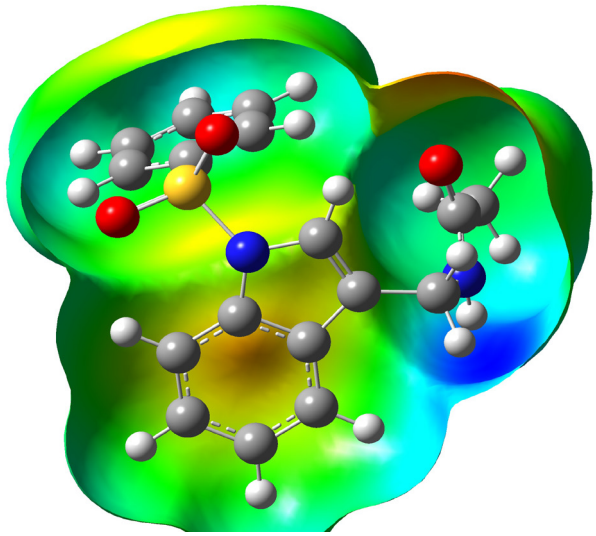

Figure 4: Molecular electrostatic potential diagram of N-((1-(phenylsulfonyl)-1H-indol-3-yl)methyl)acetamide.

Atoms	Charges	Atoms	Charges	Atoms	Charges	Atoms	Charges
C1	0.577027	C11	-0.087666	C21	-0.072860	H31	0.072460
C2	-0.395454	C12	-0.110949	C22	-0.096736	H32	0.090540
O3	-0.524224	C13	-0.088301	C23	-0.076653	H33	0.094154
N4	-0.503771	C14	0.261516	H24	0.108536	H34	0.125605
C5	-0.124109	S15	1.253532	H25	0.145389	H35	0.136340
N6	-0.687428	O16	-0.533908	H26	0.147683	H36	0.111008
C7	0.065181	O17	-0.533867	H27	0.262419	H37	0.108324
C8	0.044685	C18	-0.177122	H28	0.135455	H38	0.108456
C9	0.066036	C19	-0.078796	H29	0.110786	H39	0.148693
C10	-0.152691	C20	-0.085473	H30	0.156182	-	-

Table 4: Population analysis of N1PS3MA calculated by B3LYP/6-311++G(d,p) basis set.

$$\eta = \frac{I - A}{2},\ \mu = \frac{-(1 + A)}{2},\ \chi = \frac{I + A}{2},\ S = \frac{1}{\eta}$$

The values obtained for those global reactivity descriptors are listed in Table 5. For visual comparison the HOMO and LUMO diagram of the compound is shown in Figure 7.

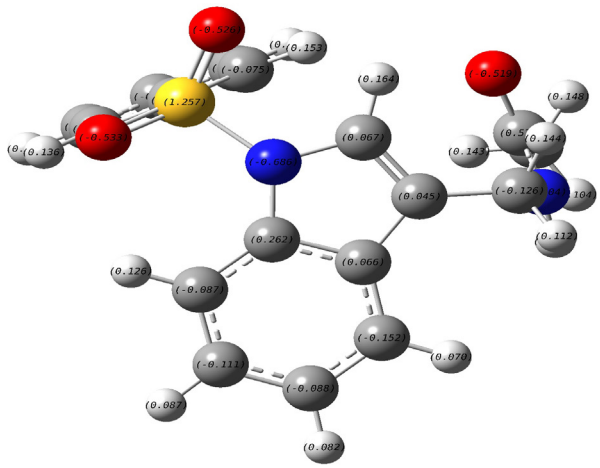

Figure 5: Mulliken atomic charges diagram of N-((1-(phenylsulfonyl)-1H-indol-3-yl)methyl)acetamide.

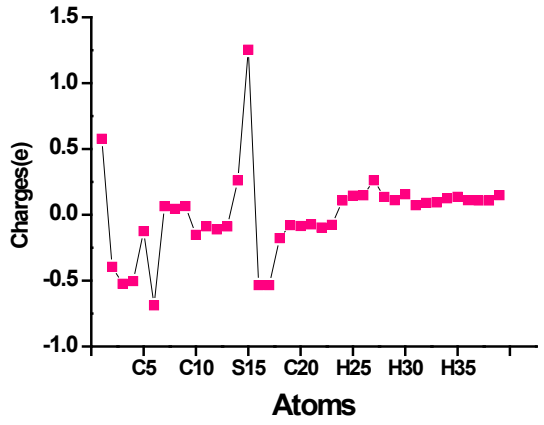

Figure 6: Mulliken atomic charge versus atom diagram of N-((1-(phenylsulfonyl)-1H-indol-3-yl)methyl)acetamide.

Thermodynamic parameters

The temperature dependence of the thermodynamic properties such as heat capacity at constant pressure (Cp), entropy (S) and enthalpy change ($\Delta H_{0 \to T}$) [40] for N1PS3MA were also determined by B3LYP/6-311++G(d,p) method and listed in Table 6. The Figure 7 depicts the correlation of heat capacity at constant pressure (Cp), entropy (S) and enthalpy change ($\Delta H_{0 \to T}$) with temperature and the corresponding fitting equations are as follows

$S^{o}m = 240.03433 + 0.7328\ T - 1.79433 \times 10^{-4}\ T^{2}\ (R^{2} = 0.9999)$

$C^{o}pm = 15.26587 + 0.65639\ T - 2.82786 \times 10^{-4}\ T^{2}\ (R^{2} = 0.9998)$

$H^{o}m = -7.65942 + 0.08696\ T + 1.73344 \times 10^{-4}\ T^{2}\ (R^{2} = 0.9998)$

The entropies, heat capacities, and enthalpy changes are increasing with temperature ranging from 100 to 1000 K due to the increase in vibrational intensities with temperature. For the title compound, all thermodynamic parameters have been increased steadily.

Molecular properties	B3LYP/6-311++G(d,p)	B3LYP/6-31G(d,p)	Molecular properties	B3LYP/6-311++G(d,p)	B3LYP/6-31G(d,p)
εHOMO(eV)	-5.88668	-6.32696	Chemical hardness(η)	2.31598	2.5002
εLUMO(eV)	-1.25472	-1.32656	Chemical potential(μ)	-3.57071	-3.8267
ε(H-L) (eV)	4.63195	5.00042	Electronegativity (χ)	3.57071	3.8267
Ionization potential(I)	5.88668	6.32696	Electrophilicity index(ω)	6.37498	7.3218
Electron affinity(A)	1.25472	1.32656	Softness(S)	0.43178	0.3999

Table 5: Molecular properties of N1PS3MA.

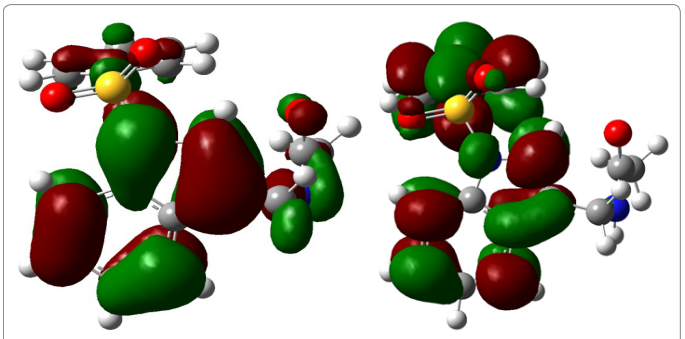

Figure 7: HOMO-LUMO energy diagram of N-((1-(phenylsulfonyl)-1H-indol-3-yl)methyl)acetamide.

T (K)	S (J/mol.K)		Cp (J/mol.K)		ddH (kJ/mol)	
	6-31G(d,p)	6-311++G(d,p)	6-31G(d,p)	6-311++G(d,p)	6-31G(d,p)	6-311++G(d,p)
100	406.32	401.71	136.67	141.78	11.42	9.17
200	526.35	528.66	227.69	236.69	24.16	28.03
298.15	642.01	641.59	338.55	335.83	61.32	56.11
300	734.23	733.68	360.07	357.69	65.99	69.73
400	818.73	810.16	438.21	432.96	105.97	99.37
500	889.56	888.72	505.6	513.42	153.26	146.82
600	953.98	959.28	561.23	578.34	201.82	197.53
700	1051.25	1052.5	616.77	630.53	263.14	258.06
800	1141.3	1139.56	664.38	673.05	327.19	323.31
900	1224.85	1220.93	701.83	708.23	393.76	392.43
1000	1302.62	1297.12	732.4	737.72	462.11	464.77

Table 6: Thermodynamic parameters of N1PS3MA.

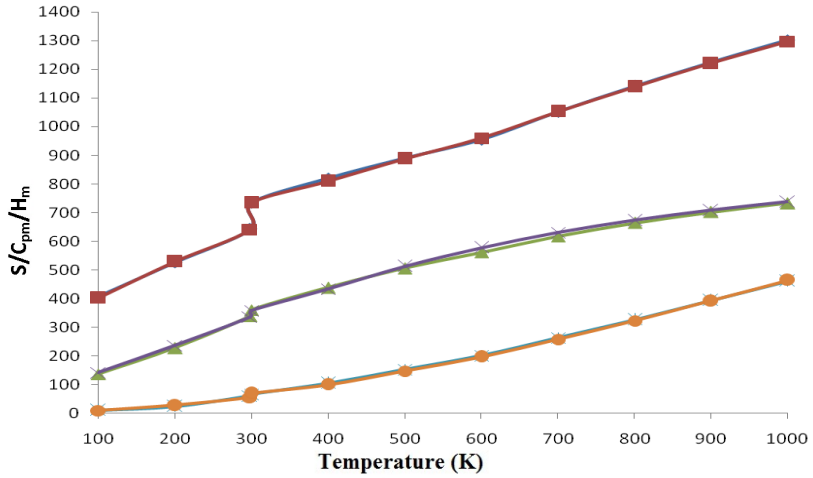

Figure 8: Thermodynamical parameters of N-((1-(phenylsulfonyl)-1H-indol-3-yl)methyl)acetamide.

Conclusion

The vibrational FT-IR and FT-Raman spectra of N1PS3MA were recorded and computed vibrational wavenumbers and their PED were calculated. The molecular structural parameters like bond length, bond angles, thermodynamic properties and vibrational frequencies of the fundamental modes of the optimized geometry have been determined from DFT calculations using 6-31G (d,p) and 6-311++G(d,p) basis sets. NBO analysis was made it indicated the intra molecular charge transfer between the bonding and antibonding orbital's. The calculated HOMO and LUMO energies were used to analyse the charge transfer within the molecule. With the help of HOMO, LUMO values, the global reactivity descriptors were calculated. The predicted MEP Figure 8 revealed the negative regions of the molecule was subjected to the electrophilic attack of this compound.

References

1. Quetin-Leclercq J (1994) Potential anticancer and antiparasitic indole alkaloids. J Pharm Belg 49: 181-192.
2. Mukhopadhyay GA, Handy S, Funayama GA, Cordell S (1981) Anticancer indole alkaloids of Rhazya stricta. J Nat Prod 44: 696-700.
3. Taylor DL, Ahmed PS, Chambers P, Tyms AS, Bedard J, et al. (1999) Pyrido [1,2a] indole derivatives identified as novel non-nucleoside reverse transcriptase inhibitors of human immunodeficiency virus type 1. Antiviral Chem Chemother 10: 79-86.
4. Williams TM, Ciccarone TM, MacTough SC, Rooney CS, Balani SK, et al. (1993) 5-chloro-3- (phenylsulfonyl)inodole-2-carboxamide:a novel, non-nucleoside inhibitor of HIV-1 reverse transcriptase. J Med Chem 36: 1291-1294.
5. Sivaraman J, Subramanian K, Velmurugan D, Subramanian E, Seetharaman J (1996) X-ray structure of 3-phenylthio-2-[1'-phenylsulfonyl-2'(3-pyridyl)vinyl) indole and its interaction with calf thymus DNA by spectroscopic methods. J Mol Struct 385: 123-128.
6. Thenmozhi S, SubbiahPandi A, Dhayalan V, MohanaKrishnan AK (2009) N-[(3-phenylsulfanyl-1-phenylsulfonyl-1H-indol-2-yl)methyl]acetamide. Acta Cryst 65: 1020-1021.
7. Frisch MJ, Trucks GW, Schlegel HB, Scuseria GE, Robb MA, et al. (2004) People Gaussian 03W Program. Gaussian Inc., Wallingford, CT.
8. Becke D (1993) Density-functional thermochemistry–III, the role of exact exchange. J Chem Phys 98: 5648-5652.
9. Lee C, Yang W, Parr RG (1988) Development of the colle-salvetti correlation-energy formula into a functional of the electron density. Phys Rev 37: 785-789.
10. John Xavier R, Ashok Raj S (2013) Ab initio, density functional computations, FT–IR, FR, Raman and molecular geometry of 4-morpholine carbonitrile. Spectrochimica Acta 101: 148-155.
11. Rajamani T, Muthu S, Karabacak M (2013) Electronic absorption, vibrational spectra, nonlinear optical properties, NBO analysis and thermodynamic properties of N-(4-nitro-2-phenoxyphenyl) methanesulfonamide molecule by ab initio HF and density functional methods. Spectrochimica Acta 108: 186-196.
12. Muthu S, Prasath M, Arun Balaji R (2013) Experimental and theoretical investigations of spectroscopic properties of 8-chloro-1-methyl-6-phenyl-4H-[1,2,4]triazolo[4,3-a][1,4]benzodiazepine. Spectrochim Acta 106: 129-145.
13. Ramachandran G, Muthu S, Renuga S (2013) Quantum mechanical study of the structure and spectroscopic (FT-IR, FT-Raman), first-order hyperpolarizability, NBO and HOMO–LUMO analysis of S-S-2-methylamino-1-phenyl propan-1-ol. Spectrochim Acta 107: 386-398.
14. Parimala K, Balachandran V (2013) Structural study, NCA, FT-IR, FT-Raman spectral investigations, NBO analysis and thermodynamic properties of 20,40-difluoroacetophenone by HF and DFT calculations.
15. Emilio L, Deigo MG, Gustavo AE, Oscar EP, Cesar ANC, et al. (2014) Synthesis, Crystal structure, conformational and vibrational properties of 6-acetyl-2,2-dimethyl-chromane. Spectrochim Acta Part A 127: 74-84.
16. Umamaheswari J, Muthu S, Tom S (2013) An experimental and theoretical study of the vibrational spectra and structure of Isosorbide dinitrate.
17. Sajan D, Ravindra HJ, Neeraj M, Joe IH (2010) Intramolecular charge transfer and hydrogen bonding interactions of nonlinear optical material N-benzoyl glycine: Vibrational spectral study. Vib Spectrosc 54: 72-80.
18. Tsuboi M (1960) 15N isotope effects on the vibrational frequencies of aniline and assignments of the frequencies of its nh2 group. Spectrochim Acta 16: 505-512.
19. Singh NP, Yadav RA (2001) Optics and spectroscopy-vibrational studies of trifluoromethyl benzene derivatives I: 2-amino, 5-chloro and 2-amino, 5-bromo benzotrifluorides. Indian Journal of Physics and Proceedings of the Indian Association for the Cultivation of Science-B 75: 347-356.
20. Silverstein M, Basseler GC, Morill C (1981) Spectrometric identification of organic compounds. Wiley, NY, USA.
21. Gnanasambandan T, Gunasekaran S, Seshadri S (2013) The spectroscopic (FTIR, FT Raman and UV-Vis spectra), DFT and normal coordinate computations of m- nitromethylbenzoate. Spectrochim Acta A 112: 52-61.
22. Lin-Vein D, Colthup NB, Fateley WG, Grasselli JG (1991) The Handbook of Infrared and Raman Characteristic Frequencies of Organic Molecules, Academic Press, San Diego, USA.
23. Amalanathan M, Joe IH, Kastova I (2009) Density functional theory calculation and vibrational spectral analysis of 4-hydroxy-3-(3-oxo-1-phenylbutyl)-2H-1-benzopyran-2-one. J Raman Spectrosc 41: 1076-1084.
24. Sharma YR (1993) Elementary Principles and Chemical Applications, S. Chand and Company Ltd., New Delhi, India.
25. Keresztury G, Chalmers JM, Griffiths PR (2002) Raman spectroscopy: Theory in Hand book of vibrational spectroscopy. Vol. I, John Wiley and Sons.

26. Roeges NPG (1994) A guide to complete interpretation of Infrared spectra of organic structures. Wiley: NY, USA

27. Varsanyi G (1969) Vibrational spectra of benzene derivatives. Academic Press, NY, USA.

28. Green JHS, Harrison DJ, Kynaston W (1971) Vibrational spectra of benzene derivatives—XIV. Spectrochim Acta 27A: 2199-2217.

29. Sundaraganesan N, Joshua BD, Mani P, Jayaprakash A, Meganathan C (2008) Molecular structure and vibrational spectra of 3-chloro-4-fluoro benzonitrile by ab initio HF and density functional method. Spectrochim Acta A 71: 1134-1139.

30. Socrates G (2000) Infrared characteristic group frequencies. John Wiley, NY, USA.

31. Seshadri S, Gunasekaran S, Muthu S (2009) Vibrational spectroscopic investigation using ab initio and dft studies on diazoxide. J Raman Spectroscopy 40: 639-644.

32. Gnanasambandan T, Gunasekaran S, Seshadri S (2014) DFT computations and spectroscopic analysis of p-bromoacetanilide. Spectrochimi Acta A 122: 542-552.

33. Reed AE, Schleye PVR (1988) The anomeric effect with central atoms other than carbon. 2. Strong interactions between nonbonded substituents in mono- and polyfluorinated first- and second-row amines, FnAHmNH2. Inorg Chem 27: 3969-3987.

34. Xavier RJ, Gobinath E (2012) Density functional theory study on characterization of 3-chloro-1,2-benzisothiazole. Spectrochim. Acta A 91: 248-255.

35. Gupta VP, Sharma A, Virdi V, Ram VJ (2006) Structural and spectroscopic studies on some chloropyrimidine derivatives by experimental and quantum chemical methods. Spectrochim Acta Part A 64: 57-67.

36. Gnanasambandan T, Gunasekaran S, Seshadri S (2014) Experimental and theoretical study of p-nitroacetanilide. Spectrochimica Acta 117: 557- 567.

37. Parthasarathi R, Padmanabhan J, Elango M, Subramanian V, Chattaraj P (2004) Intermolecular reactivity through the generalized philicity concept. Chem Phys Lett 394: 225-230.

38. Parthasarathi R, Padmanabhan J, Subramanian V, Maiti B, Chattaraj P (2004) Toxicity analysis of 33'44'5-pentachloro biphenyl through chemical reactivity and selectivity profiles. Curr Sci 86: 535-542.

39. Parthasarathi R, Padmanabhan J, Subramanian V, Sarkar U, Maiti B (2003) Toxicity analysis of benzidine through chemical reactivity and selectivity profiles: a DFT approach, Internet Electron. J Mol Des 2: 798-813.

40. Irikura KK (2002) THERMO.PERL Script. National Institute of Standards and Technology.